v. 3, n. 22, 2023

Journal of
Engineering
Research

METHOD FOR REDUCING SIDELOBE INTERFERENCE IN WATER COLUMN DATA ACQUIRED BY MULTIBEAM ECHOSOUNDERS

Haroldo Júnio dos Santos
Universidade de Brasília, Electrical Engineering Department
Brasília – DF
https://lattes.cnpq.br/9884195612470734

Luciano Emídio Neves da Fonseca
Universidade de Brasília, Faculty of Electronic Engineering - FGA
Brasília – DF
http://lattes.cnpq.br/8651274159440619

Ricardo Lopes de Queiroz
Universidade de Brasília, Computer Science Department
Brasília – DF
http://lattes.cnpq.br/9271885452744905

Abstract: In underwater remote sensing, the acoustic waves emitted by multibeam echo sounder interact with the existing medium though the wave path from the transducer towards the seafloor, mainly with its discontinuities (in acoustic impedance), both in the water column and at the seafloor. The proper measuring of the water column scatterers and reflections can help mapping important environmental properties in water bodies. Nevertheless, the seafloor, which poses the strongest impedance contrast, reflects and absorbs these wave fronts, causing measurement errors at the water column. Due to the acoustic beam geometry and spatial pattern, sidelobes are also reflected by the seafloor, causing strong constructive interference with the main lobe reflection, mainly at distances greater than the length of the central beam. For this reason, an *SRSN* algorithm is proposed to reduce this interference, leading to satisfactory results. Experimental data acquired in the Celtic Sea using an EM2040 multibeam echo sounder are used to validate the proposed algorithm.
Keywords: interference, water column, multibeam echo sounder

INTRODUCTION

Modern multibeam echo sounder (MBES) can acquire bathymetry and acoustic backscatter data from the seafloor, in the form of time series of acoustic samples, from multiple beams at different angles (Lurton et al., 2015). However, the capabilities of MBES are not limited to the seafloor, they can also record acoustic samples from the water column. The information available in the water column can be used to determine fishing locations (L. Mayer, 2002), oil and, mainly, gas leaks in potential oil deposits (P. Urban et al., 2017) and pipelines (J. Agbakwuru, 2012), hydrothermal vents (K. Nakamura et al., 2015), underwater objects and shipwrecks (C. Marques et al., 2012) and marine flora (Schimel, A. C. et al., 2020).

MBES acquisitions have different types of noise sources, but the one that causes the most problems are the sidelobes (Clarke, J. H., 2006). Due to the beam patterns characteristics of the transmit and receive arrays, sidelobes are generated, which interact with strong acoustic targets on the water column, and their reflections create interference, generating artifacts around these targets (Schimel, A. C. et al., 2020). This type of interference is always present in MBES acquisitions and it is necessary to apply data processing and filtering techniques in order to remove it.

The MBES records are stored in asynchronous binary datagram formats, which can be easily parsed and interpreted. Each datagram stores specific data such as position, backscatter, water column data, etc. (H. dos Santos and B. de Souza, 2018). With a proper time-tag, it is possible to correlate two or more datagrams, such as the positioning, the depth or even the *backscatter* datagrams.

METHODS

SLANT-RANGE SIGNAL NORMALIZATION

The interference caused by sidelobes is much more intense at distances greater than the depth of the central beam and it has a tendency to homogeneous for the same radial distance. For this reason, a slant-range signal normalization (SRSN) algorithm can be used to reduce interference, by decreasing the intensity level, at all distances, to an equivalent average level. For that, it applies an adaptive data processing technique, which takes into account into consideration the global and local water column statistics. The developed algorithm is an adaptation of the technique proposed by Schimel, A. C. et al (2020), where the average of the samples in the same radial

distance is subtracted and the average of the samples of the 11 most central beams is added (Equation, number 1). The central beams are considered more important, as they are subject to less interference.

Originally the algorithm calculated the average by multiplying the data to a rectangular window of size 11 centered on the central beam. An adaptation was performed in which the mean is calculated by multiplying the data to a Gaussian window centered on the central beam, thus considering all beams with a certain degree of importance proportional to the distance from the central beam.

$$BS_f(P,B,S) = BS_o(P,B,S) - \frac{1}{N_B}\sum_{b=1}^{N_B} BS_o(P,b,S) + \frac{1}{11N_S(P)}\sum_{s=1}^{N_S(P)}\sum_{b=\frac{N_B}{2}-5}^{\frac{N_B}{2}+5} BS_o(P,b,s) \quad (1)$$

Where BS_f and BS_o are respectively the filtered and the original *backscatter* values for the *ping P*, beam *B* and sample *S*. N_B is the number of beams, and $N_S(P)$ is the sample number corresponding to the *bottom detect* for the center beam in the *ping P* (Schimel, A. C. et al, 2020).

A Gaussian distribution with a mean μ and variance σ^2 can be calculated from Eq.2.

$$W(n|\mu,\sigma^2) = \frac{1}{\sqrt{2\pi\sigma^2}} exp\left[-\frac{1}{2}\left(\frac{n-\mu}{\sigma^2}\right)^2\right] \quad (2)$$

For the calculation of the window, the average μ is the number of the central beam, and the standard deviation σ^2 is 5% the total number of beams.

FOURIER TRANSFORM

Assuming that the desired signal and the noisy interference are independent in frequency, it is possible to detect and reduce the interference by using processing techniques in the frequency domain, applying a *Fast-Fourier Transform* (FFT).

First, the FFT of the portion of the signal where the interference is less significant is taken. After that, the FFT of the rest of the signal is taken. The aim is to make the frequency responses of both portions similar by filtering out spurious frequency components.

PROCESSING IN THE SPATIAL DOMAIN

In addition to the frequency-domain techniques shown above, the use of spatial filters can be effective in reducing noise and interference (J. Jaybhay and R. Shastri, 2015). Adaptive median and alpha-trimmed mean filters were proposed.

In the median adaptive filter, the median and the 1st and 9th deciles of a NxN pixel neighborhood are taken. If the value of the central pixel of the neighborhood is lower than the 1st decile, or higher than the 9th decile, it is replaced by the median.

In the adaptive alpha-trimmed mean filter, the average of the central values, from αN^2 to $(1-\alpha)N^2$ ordered pixels from a neighborhood of NxN pixels of the image, is taken. The center pixel value is then substituted for this average.

MOUNTING THE WATER COLUMN GRIDS

For a better geolocation of the data, the latitude and longitude values are converted from WGS84 to UTM (converted from degrees to meters around a central meridian), using the proper UTM zone for the location of the data. The position data is then interpolated by the time it was acquired. With this interpolation it is possible to locate the water column datagrams, as well as those of bathymetry, backscatter, sound velocity profile, etc.

To assemble each frame, it is necessary to use the angles of arrival of all beams, together with the sampling rate and the speed of sound. The distance between each sonar sample can be calculated using Eq. 3 and 4 and the

positions x and y with respect to the sonar with Eq. 5 and 6, respectively. These equations are needed for ray-tracing compensation.

$$\theta_n = arcsin\left(\frac{v_n}{v_{n-1}} \times sin(\theta_{n-1})\right) \quad (3)$$

$$d_n = \frac{v_{sn}}{2 \times f_s} \quad (4)$$

Where, θ_n is the angle in the sample *n*, d_n is the distance between the samples, v_{sn} the speed of sound in the sample *n* e fs the sampling frequency.

$$x_n = \sum_{k=1}^{n} \sin(\theta_k) \times d_k \quad (6)$$

$$y_n = \sum_{k=1}^{n} \cos(\theta_k) \times d_k \quad (7)$$

Where x_n and y_n are the coordinates of sample *n* relative to the sonar.

RESULTS

The data used for these analyses were acquired in February 2013 in the Celtic Sea, off the coast of France [Fig. 1], by a multibeam sonar model EM2040, which has an operating frequency between 200 kHz and 400 kHz, survey capability in depths from 0.5 to 600 meters and maximum configurable beam resolution of 0.4°x0.7° (Kongsberg, 2013).

SLANT-RANGE SIGNAL NORMALIZATION (SRSN)

First it is necessary to create a grid and insert all the acoustic samples for the transducer the seafloor, using for that the sample number obtained from the *bottom detection* as a reference for the seafloor. The data are quantified in bins and the median is taken for each *bin*. The result is the image shown in Fig. 2.

It is important to note that there is strong interference caused by sidelobes in the form of semi-circles at the area beyond a certain radius distance between the sonar and the seafloor. We could focus the analyzes to the portion of the signal not strongly affected by this type of interference, by using only data closer than a certain radius between the sonar and the seafloor. However, using only this portion of the data can result in significant loss, especially when it is crucial to analyze the region close to the seafloor. To ensure that potentially useful data is not discarded, the SRSN algorithm was used. The result is present in Fig. 3.

FOURIER TRANSFORM

The filtering technique in the frequency domain is applied by comparing the FFT of the part of the signal where there is not much interference (Fig. 5) to the FFT of the rest of the signal (Fig. 4). The filtered data is shown in Fig. 6.

The used filter applies a windowing technique based on the difference between the FFT of the signal with less interference and the FFT of the complete signal.

The Inverse Fourier Transform (IFFT) of the filtered signal is shown in Fig. 7. A reduction in interference is observed, along with an amplification of the desired signal without degrading information.

Another approach applied to the signal was to take the average of the FFT of 10 *frames* around the current *frame* and subtract it from the signal FFT. The result is shown in Fig. 8.

PROCESSING IN THE SPATIAL DOMAIN

For the implementation of the adaptive median filter, a 9x9 neighborhood was used to calculate the local statistics. The result can be seen in Fig. 9.

For the implementation of the alpha-trimmed mean filter, a 3x3 neighborhood and a factor $\alpha = 0.2$ were used to calculate the local statistics. The result can be seen in Fig. 10.

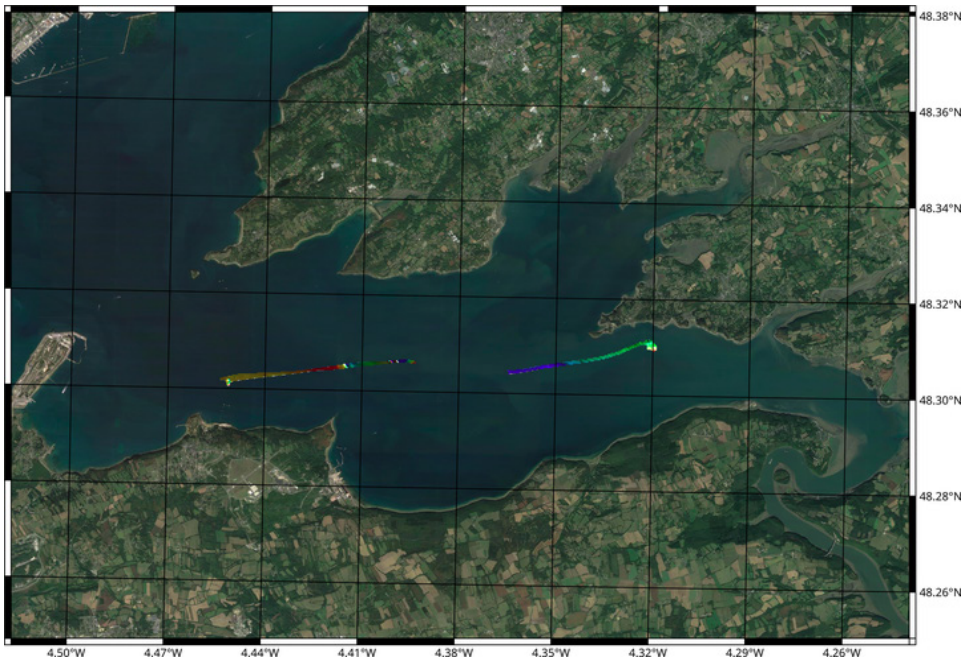

Figure 1 – Survey area. Celtic Sea, coast of France.

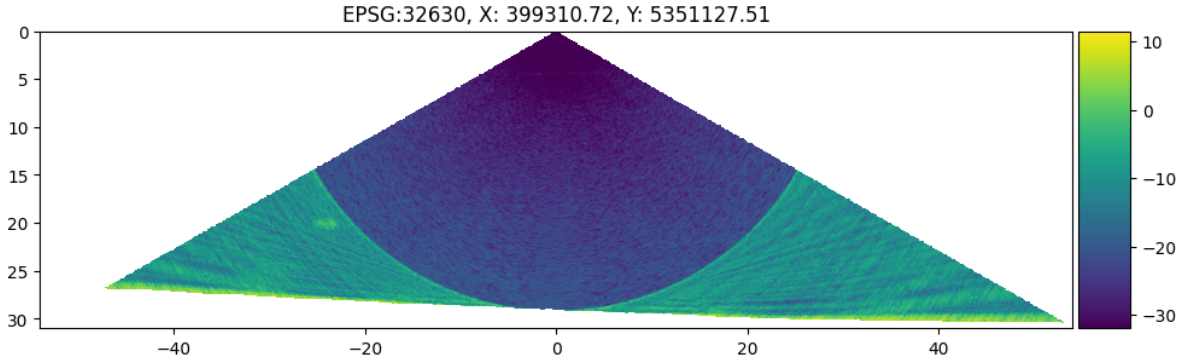

Figure 2 - Grid mounted with time series samples down to the floor.

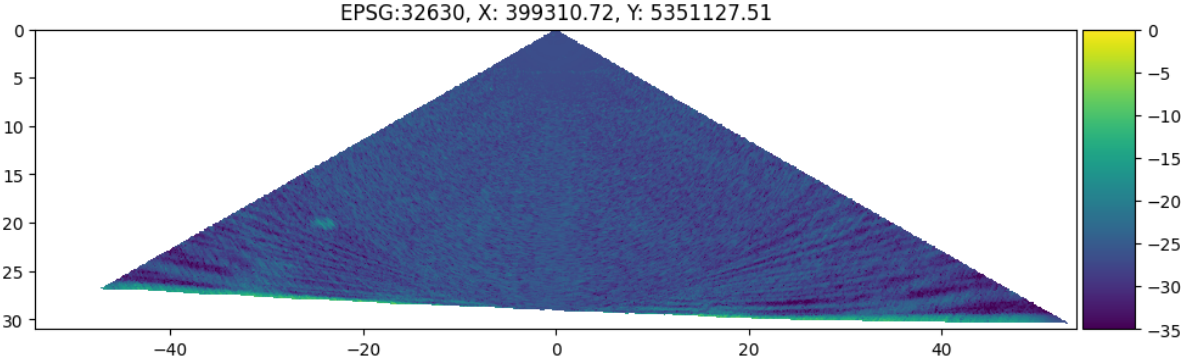

Figure 3 - Grid mounted with time series samples using SRSN algorithm with Gaussian window.

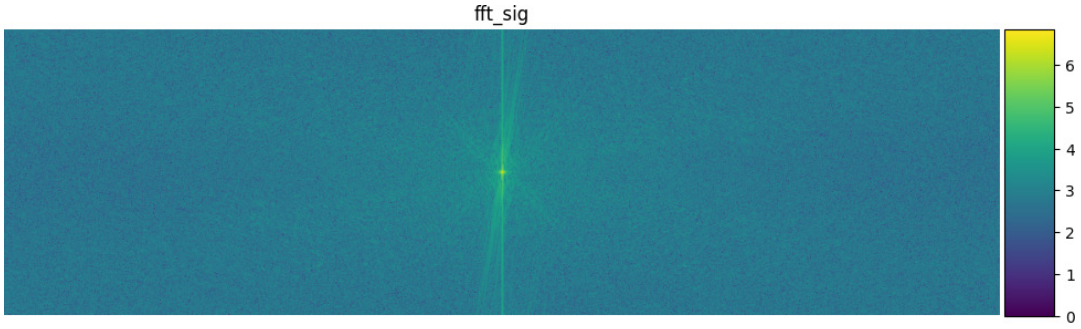

Figure 4 - FFT of the signal.

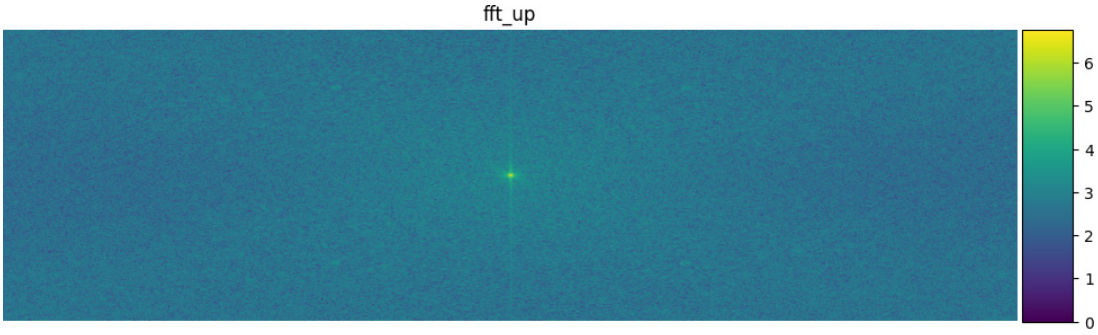

Figure 5 - FFT of the portion of the signal where the interference is less significant.

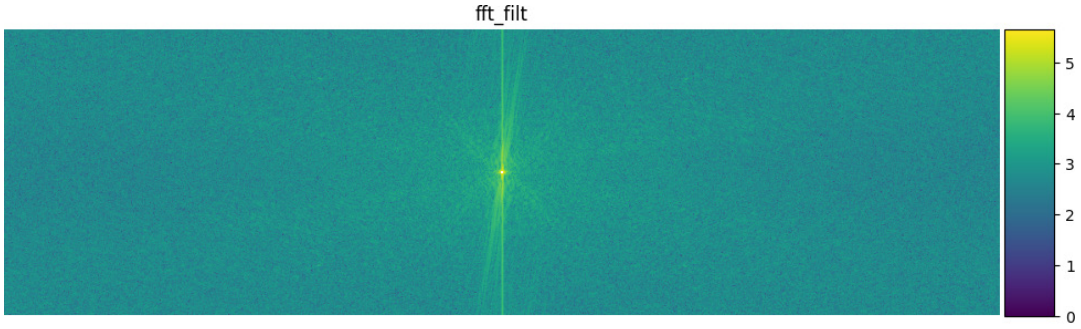

Figure 6 - FFT of the filtered signal.

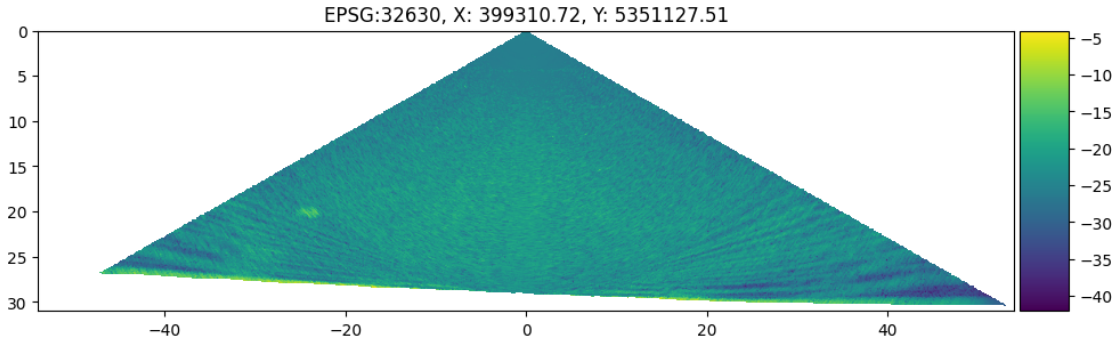

Figure 7 - IFFT of the filtered signal.

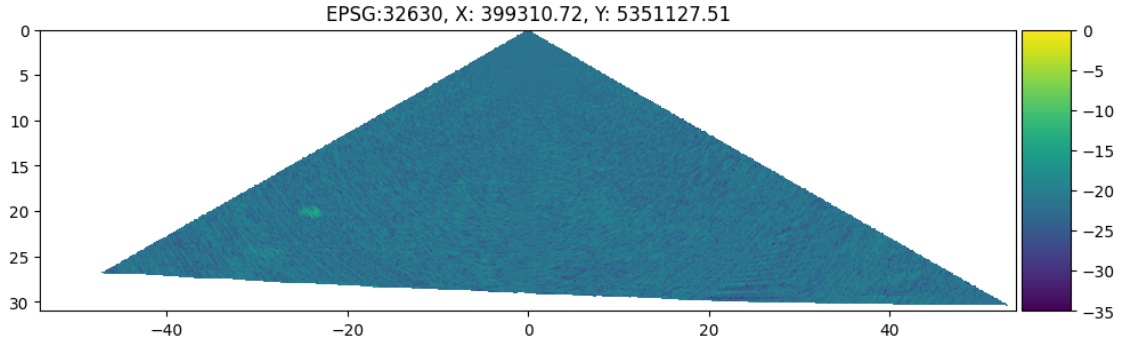

Figure 8 – IFFT of the signal subtracted from the average of the part of the signal where the interference is less significant in 10 frames.

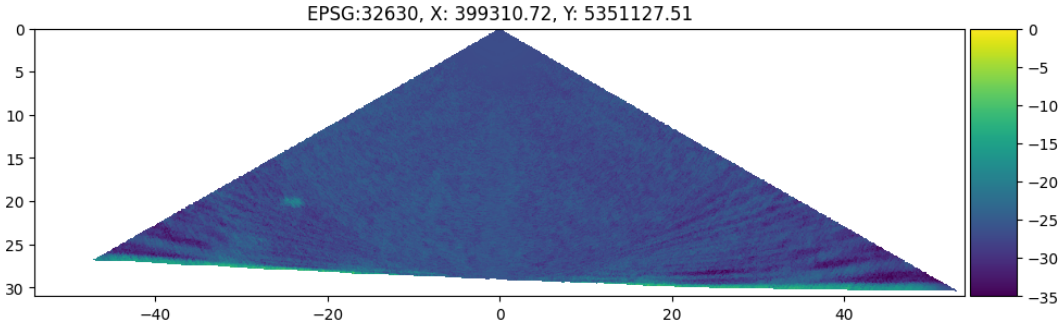

Figure 9 – Filtered image with adaptive median filter.

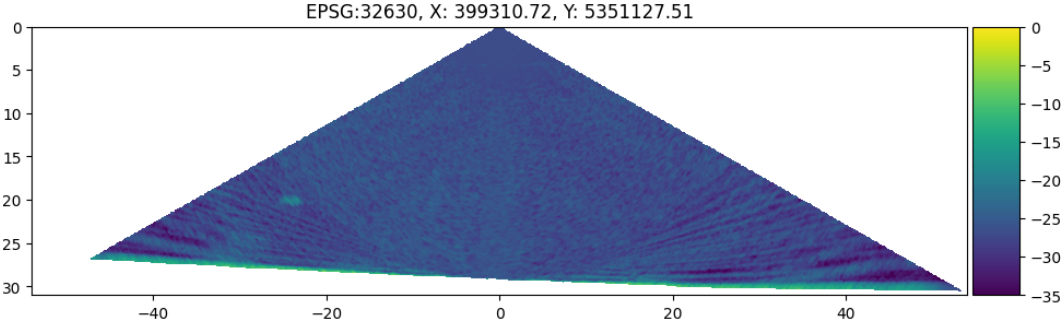

Figure 10 – Filtered image with alpha pruned adaptive mean filter.

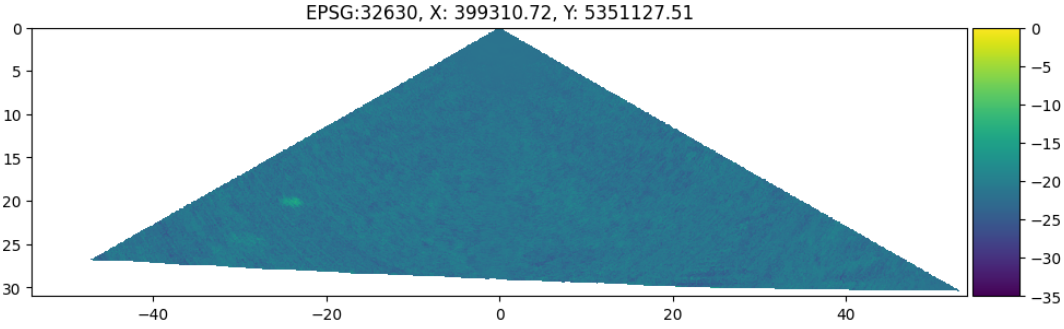

Figure 11 - Filtered image using the frequency domain technique and the adaptive median filter.

COMBINATION OF BOTH TECHNIQUES

A combination of the interference and the *speckle* noise reductions can be achieved by applying the adaptive median filter to the filtered image in the frequency domain shown in Fig. 8. The result can be seen in Fig. 11.

CONCLUSION

Sidelobe interference greatly degrades water column data acquired by multibeam echo sounders. The techniques proposed to reduce interference made it possible to recover part of the data, even in places with highly degraded signals. By applying a combination of frequency domain filters (to reduce strong interferences near the seafloor) and spatial filters (to normalize the signals and reduce *speckle* noise), it is possible to utilize information that otherwise could not be used.

It was observed a great reduction of the interference caused by the secondary sidelobes after the application of the proposed SRSN algorithm and the proposed frequency domain filter. However, when using only median or alpha-trimmed filters, no significant reduction in interference was detected, especially in the alpha-trimmed mean filter. With the combination of both filters, the resulting signal is greatly improved.

REFERENCES

Agbakwuru, J. (2012). Oil/Gas pipeline leak inspection and repair in underwater poor visibility conditions: challenges and perspectives. *Journal of Environmental Protection*, *2012*.

Clarke, J. H. (2006). Applications of multibeam water column imaging for hydrographic survey. Hydrographic Journal, 120, 3.

dos Santos, H. J., & de Souza, B. M. (2018). Desenvolvimento de metodologias de quantização espacial para o processamento de sinais de retroespalhamento acústico e batimetria adquiridos por sonares multifeixe. *BDM Universidade de Brasília*.

Jaybhay, J., & Shastri, R. (2015). A study of speckle noise reduction filters. S*ignal & Image processing: An international Journal (SIPIJ)*, *6*(3), 71-80.

Kongsberg, "Application note: Discovering the redefined EM multibeam series," 2013.

Lurton, X., Lamarche, G., Brown, C., Lucieer, V., Rice, G., Schimel, A. and Weber, T. (2015). Backscatter measurements by seafloor-mapping sonars - Guidelines and Recommendations.

Marques, C. (2012). Automatic mid-water target detection using multibeam water column. *UNB Scholar*.

Mayer, L., Li, Y., & Melvin, G. (2002). 3D visualization for pelagic fisheries research and assessment. *ICES Journal of Marine Science*, *59*(1), 216-225.

Moszynski, M., Chybicki, A., Kulawiak, M., & Lubniewski, Z. (2013). A novel method for archiving multibeam sonar data with emphasis on efficient record size reduction and storage. *Polish Maritime Research*, *20*(1), 77-86.

Nakamura, K., Kawagucci, S., Kitada, K., Kumagai, H., Takai, K., & Okino, K. (2015). Water column imaging with multibeam echo-sounding in the mid-Okinawa Trough: Implications for distribution of deep-sea hydrothermal vent sites and the cause of acoustic water column anomaly. *Geochemical Journal*, *49*(6), 579-596

Schimel, A. C., Brown, C. J., & Ierodiaconou, D. (2020). Automated filtering of multibeam water-column data to detect relative abundance of giant kelp (Macrocystis pyrifera). *Remote Sensing*, *12*(9), 1371.

Urban, P., Köser, K., & Greinert, J. (2017). Processing of multibeam water column image data for automated bubble/seep detection and repeated mapping. *Limnology and oceanography: methods*, *15*(1), 1-21.